Proceedings of ICRC 2001: 1375 © Copernicus Gesellschaft 2001

ICRC 2001

Energy distribution of produced particles in multiple particle production based on data of direct observation

A. Ohsawa[1], **E. H. Shibuya**[2], **and M. Tamada**[3]

[1]Institute for Cosmic Ray Research, University of Tokyo, Kashiwa, Chiba, 277-8582 Japan.
[2] Instituto de Fisica Gleb Wataghin, Univ. Estadual de Campinas, 13083-970 Campinas, São Paulo, Brasil.
[3]Faculty of Science and Technology, Kinki University, Higashi-Osaka, Osaka, 577-8502 Japan.

Abstract. The energy distribution of produced particles in *multiple particle production* is formulated empirically based on the data of direct observations by accelerator and cosmic-ray experiments at $10^{12} \sim 10^{14}$ eV. The formulated distribution indicates violation of the Feynman scaling law, which was shown to be valid in low energy region of $\leq 10^{12}$ eV. That is, the particle density is suppressed in the forward region and enhanced in the central region, compared with the distribution of the Feynman scaling law. Consequences of the formulated distribution, such as multiplicity, inelasticity, etc., are discussed at high energies of $\geq 10^{15}$ eV by extrapolation. The distribution is also compared with those of nuclear interaction models which are used widely in simulations of accelerator and cosmic-ray experiments.

1 Introduction

To discuss multiple particle production (MPP) it is convenient to start from the energy distribution of produced particles, since some important features of MPP, such as inelasticity and multiplicity, are derived from it. To discuss the energy distribution, however, we have almost no $a\ priori$ guiding principles except energy conservation. Hence it may be reasonable to take a phenomenological approach or to start from experimental data while as much as possible trying to avoid assumptions without experimental basis.

Our study is made in the following way. Assuming the energy distribution of produced particles, which tends to that of the Feynman scaling law at low energies, we determine magnitudes of the scaling violation parameters at various collision energies where the experimental data is available. Assuming that the obtained energy dependence of the scaling violation parameters is valid up to 10^{20} eV, we discuss the consequences of the formulated distribution at higher energies. The formulated distribution is compared with the predictions of models which are used widely in simulations in accelerator and cosmic-ray experiments.

Correspondence to: A. Ohsawa
(ohsawa@icrr.u-tokyo.ac.jp)

2 Energy distribution of produced particles

In this section we discuss the energy distribution of produced particles in $N-N$ (nucleon−nucleon) inelastic collisions, under the assumption that the final state of multiple particle production consists of a surviving particle, which has the same particle nature as the incident particle, and the produced particles. The view is valid empirically if one assumes that the energy of the surviving particle is distributed between 0 and E_0 in the laboratory system. Note that the surviving particle is not always the leading particle or the highest energy particle. Plausibility of the assumption was discussed in detail (Augusto et al., 1999). This approach does not require specifying kinds of produced particles at all.

2.1 Scaling function

Feynman speculated that the energy distribution of produced particles in multiple particle production, expressed by the variable $x^* \equiv 2p^*_{||}/\sqrt{s}$ ($p^*_{||}$: the longitudinal component of the momentum vector $\boldsymbol{p}^*$ of the produced particle),[1] is independent of the incident energy $\sqrt{s}$ at high energies (Feynman, 1969). This assumption appeared to be valid up to the energy of $\sqrt{s} = 63$ GeV, the maximum available energy at that time (Taylor et al., 1976). One of the empirical formulae to express the energy distribution of *charged* produced particles is (Gaisser et al., 1978)

$$\frac{dN}{dx^*} \equiv \frac{1}{\sigma_{inel}} \frac{d\sigma}{dx^*} = D\frac{(1-x^*)^d}{x^*} \qquad (1)$$

$$(D = (d+1)/3 = 1.67, \quad d = 4.0)$$

which is called 'the scaling function'.

[1]The quantities with and without an asterisk (*) are those in the center of mass system and in the laboratory system, respectively.

2.2 Energy distribution at high energies

At still higher energies, there are several data sets of direct observation by cosmic-ray and accelerator experiments (Chinellato et al., 1983), (Alner et al., 1986), (Pare et al., 1990), (Haar et al., 1997). Note that the experimental data are presented in various quantities, such as rapidity density, pseudo-rapidity density, etc., owing to the experimental conditions of the respective groups.

To compare these data with the scaling function, one has to transform dN/dx^* into $dN/d\eta^*$, dN/dy^*, etc. In doing so, one has to take into account that the average value of the transverse momentum $< p_T >$ depends on the rapidity, $i.e.$ the value becomes smaller in the forward region (Lattes et al., 1971). Hence we assume

$$\frac{dN}{dx^* dp_T} = aD \frac{(1-a'x^*)^d}{\sqrt{x^{*2} + \left(\frac{2\mu}{\sqrt{s}}\right)^2}}\, g(p_T) \qquad (2)$$

$$(\mu \equiv \sqrt{p_T^2 + m_\pi^2})$$

where the parameters a and a' are adjustable. This formula reproduces the scaling function of eq.(1) using $a = a' = 1$ and $\sqrt{s} \to \infty$. The parameters a (≥ 1) and a' (≥ 1) express enhancement of the scaling function in the central region and suppression in the forward region, respectively.

The p_T-distribution is assumed to be

$$g(p_T)dp_T = p_T \ \exp\left(-\frac{p_T}{p_0}\right) \frac{dp_T}{p_0^2} \qquad (3)$$

with

$$p_0 = \begin{cases} c & (x^* < x_0^*) \\ c\left(\frac{x_0^*}{x^*}\right)^{c'} & (x^* > x_0^*) \end{cases} \qquad (4)$$

$$(c = 0.2 \text{ GeV}/c, \quad c' = 0.57, \quad x_0^* = 0.08)$$

According to the p_T-distribution of eq.(3), the average value of p_T, $< p_T >= 2p_0$, becomes smaller in the forward region $x^* > x_0^*$, which is observed by the experiments (Lattes et al., 1971), (Pare et al., 1990).

2.3 Scaling violation parameters

The above distribution (2) can be transformed into those of dN/dy^* and $dN/d\eta^*$ easily. Hence we can calculate the (pseudo-)rapidity density distribution at the incident energy $\sqrt{s}$ for various values of the parameters a and a', which are to be compared with those of the experimental data.[2]

We assume the energy dependence of parameter a as

$$a = \left(\frac{s}{s_0}\right)^\alpha \simeq \left(\frac{E_0}{A}\right)^\alpha \qquad (\alpha = 0.105) \qquad (5)$$

[2]The data are those of all inelastic events but not only NSD (non-single-diffractive) events. That is, $\sigma_{inel} = \sigma_{NSD} + \sigma_{SD}$.

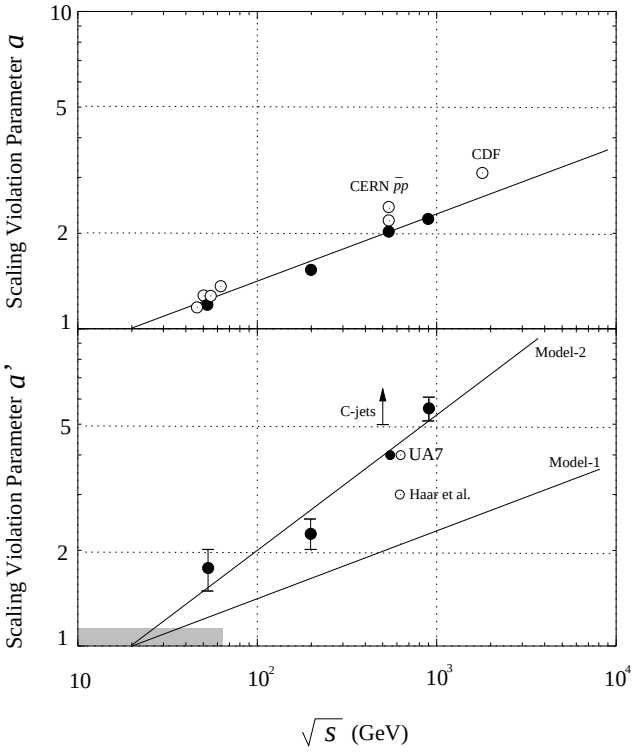

Fig. 1. Energy dependence of the scaling violation parameters, a (the upper figure) and a' (lower) in eq.(2) in the text. Plots are obtained by fitting the calculated curves of (pseudo-) rapidity density distribution to those of the experimental data. The full circles are from the experimental data of the UA5 Collaboration (Alner et al., 1986), and the open circles are from those of other experimental groups (Alner et al., 1986), (Abe et al., 1990), (Haar et al., 1997). The bar with an arrow, indicated as "C-jets", is from the cosmic-ray experiment (Chinellato et al., 1983). The hatched area indicates the energy region where the Feynman scaling law ($a \simeq 1.0$ and $a' \simeq 1.0$) is verified by the experiments. The lines are the assumed energy dependences in Model-1 and Model-2. is verified by the experiments. The lines are the assumed energy dependences in Model-1 and Model-2.

$$(s_0 = 3.9 \times 10^2 \text{ GeV}^2, \ A = 2.0 \times 10^2)$$

The energy dependence of the parameter a is shown in Fig. 1 together with experimental data. Then the pseudo-rapidity density at $\eta^* = 0$ is given by

$$\left(\frac{dN}{d\eta^*}\right)_{\eta^*=0} = D < \frac{p_T}{\mu} > a = 1.67 \times 0.83 \times \left(\frac{s}{s_0}\right)^\alpha \qquad (6)$$

which reproduces $\rho(0) = 0.74 s^{0.105}$ found by the UA5 Collaboration (Alner et al., 1986).

From the energy dependence of the parameters a and a' in Fig. 1, we assume two cases of

$$a' = \left(\frac{E_0}{A}\right)^{\alpha'} \qquad (\alpha' = 0.105 \quad \text{and} \quad 0.210) \qquad (7)$$

which are called Model-1 and Model-2 hereafter. The parameters a and a' in Model-1 have the same energy dependence,

and those in Model-2 are the best-fit to the experimental data. Note that the data from Harr *et al.* and from the C-jets of the Chacaltaya experiment deviate from the line of Model-2. Model-0 with $a = a' = 1.0$, which stands for the case of Feynman scaling law, is included for reference.

To show how the experimental data are described by the formula of eq.(2) with appropriate values of the parameters a and a', Fig. 2 presents the pseudo-rapidity density distributions of all inelastic events (but not only of non-single-diffractive events) recorded by the UA5 Collaboration together with those of the formulated models. One can see in the figure that the reproduction is satisfactory by Model-2 and that Model-0 (the Feynman scaling law) cannot reproduce the data both in the central and forward regions. Note that the distribution of Model-0 is slightly energy-dependent, as can be seen in eq.(2).

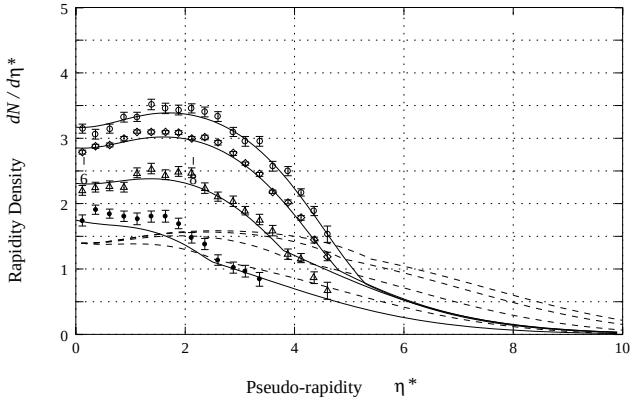

Fig. 2. Pseudo-rapidity density distributions by UA5 Collaboration experiment (plots), those of Model-2 (solid lines) and those of Model-0 (chain lines). The data are those of all inelastic events at the energies of $\sqrt{s} = 53$ GeV (•), 200 GeV (△), 546 GeV (◇), and 900 GeV (○). The solid lines are by Model-2 with the parameter values a' of the best-fitting at respective energies

3 Discussions

3.1 Multiplicity and inelasticity at high energies

Fig. 3 shows the energy dependence of charged multiplicity,

$$m(E_0) = \int_0^{1/a'} dx \int_0^{\infty} dp_T \frac{aD(1-a'x)^d}{\sqrt{x^2 + \left(\frac{2\mu}{\sqrt{s}}\right)^2}} \; g(p_T)$$

predicted by the formulated models. One can see in the figure that difference in the multiplicity is small between Model-1 and Model-2 because we have

$$m(E_0) \simeq a \left[\ln \frac{\sqrt{s}}{\mu} - \ln a' \right].$$

That is, the parameter a' appears in the form of $\ln a'$. It is no surprise that the energy dependence of Model-2 agrees better with the experimental data than that of Model-1.

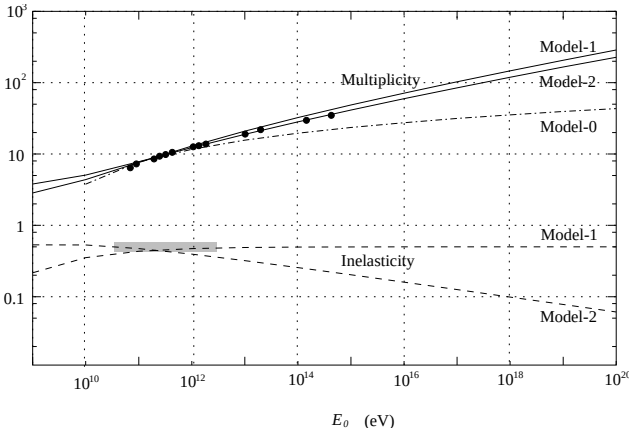

Fig. 3. Energy dependence of charged multiplicity and that of total inelasticity, predicted by the models. Experimental data of average charged multiplicity (full circles) is from bubble chambers, ISR and S$\bar{p}p$S, compiled in Ref. (Alner et al., 1986). The multiplicity is not different so much between Model-1 and Model-2. Model-2 describes the experimental data better than Model-1, because Model-2 has the best-fit parameters to describe the rapidity density distribution. Inelasticity is decreasing in Model-2, while it is constant (=0.5) for Model-0 and Model-1. The shadowed area indicates the region where the Feynman scaling law, $i.e. < K >= 0.5$, is verified by the experiments within the experimental errors.

Fig.3 shows also the energy dependence of the average total inelasticity in the laboratory system, defined by

$$< K > \equiv \frac{3}{2} \int_0^{1/a'} x dx \int_0^{\infty} dp_T \; aD \frac{(1-a'x)^d}{\sqrt{x^2 + \left(\frac{2\mu}{\sqrt{s}}\right)^2}} \; g(p_T)$$

It shows that the inelasticity decreases considerably in Model-2 at high energies while it is constant ($i.e.$ 0.5) in Model-0 and in Model-1.[3] It is worth noting that $< K >= 0.5$ holds when the relation $\alpha = \alpha'$ holds, irrespective of the values of α and α'.

3.2 Models used in simulations

It is also interesting to see how the formulated distribution is reproduced by the models which are used recently in simulations of atmospheric cosmic-ray diffusion. In Fig. 4 we compare the pseudo-rapidity density distributions (Knapp et al., 1996), predicted by UA5 code (Alner et al., 1986)[4], VENUS (Werner, 1993), QGSJET (Kalmykov and Ostapchenko, 1993) SIBYLL (Fletcher et al., 1994), HDPM (Capdevielle et al., 1992) and DPMJET (Ranft, 1995), with those of the present models. Note that the pseudo-rapidity density by simulations

[3] It may look strange that the average inelasticity $< K >$ is 0.5 for Model-1, which has a higher rapidity-density than QGSJET (See Fig. 4.), since QGSJET found $< K > \simeq 0.6$. The effect is due to the difference in sampling of events, $i.e.$ all inelastic events in the former and NSD events in the latter. In other words the average inelasticity by QGSJET is ~ 0.5 for all inelastic events.

[4] UA5 Collaboration made a simulation code which describes the data observed by the collaboration.

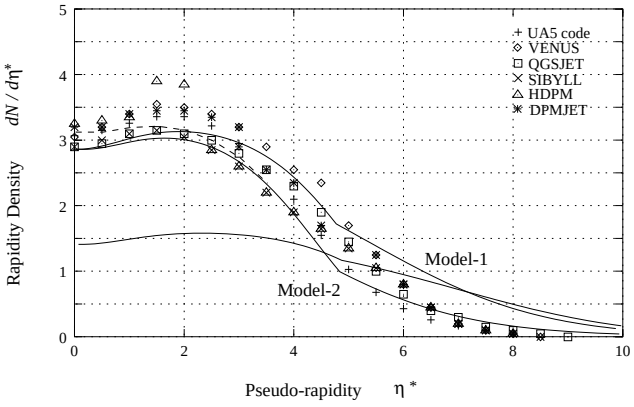

Fig. 4. Pseudo-rapidity density distributions at $\sqrt{s} = 546$ GeV. Plots are by the simulation models (UA5 code, VENUS, QGSJET, SIBYLL, HDPM and DPMJET). The data by the simulations are based on the NSD (non-single-diffractive) events, while those by Model-0, Model-1 and Model-2 (solid lines) are for all inelastic events. The chain line is that of Model-2 which is corrected for NSD events.

is for NSD (non-single-diffractive) events while that of the calculation is for all inelastic events.

The following observations can be made from Fig. 4.
(1) In the central region the distributions are similar except that of HDPM.
(2) In the middle region QGSJET, VENUS, DPMJET predict higher density appreciably than that of Model-2.
(3) In the forward region all the model predictions are almost consistent.
(4) UA5 code predicts the most consistent distribution with that of Model-2.[5]
(5) The difference of the rapidity densities, predicted by respective simulation models, is not negligibly small.
(6) The experimental data at Harr *et al.* is almost consistent with those by QGSJET. (See also the lower figure in Fig. 1.)
(7) The rapidity density of the QGSJET model, which is used frequently at present in simulations of cosmic-ray phenomena, is almost between those of Model-1 and Model-2.

References

F. Abe et al. (CDF Collaboration), Phys. Rev. **D41**(1990) 2330.
G.L. Alner et al. (UA5 Collaboration), Z. Phys. **C33** (1986) 1; Nucl. Phys. **B291** (1987) 445; Phys. Rep. Nos.5 and 6 (1987) 247.
G.J. Alner et al. (UA5 Collaboration), CERN-EP/86-213 (1986).
C.R.A. Augusto, S.L.C. Barroso, Y. Fujimoto, V. Kopenkin, M. Moriya, C.E. Navia, A. Ohsawa, E.H. Shibuya, and M. Tamada, Phys. Rev. **D61** (1999) 012003.
J.N. Capdevielle et al., Preprint of Kernforschungszentrum Karlsruhe KfK 4998 (1992).
J.A. Chinellato et al., Prog. Theor. Phys. Suppl. No.76 (1983) 1.

[5]The code does not necessarily predict the pseudo-rapidity density correctly in the forward region, because the observed pseudo-rapidity region by UA5 Collaboration is limited to $\eta^* \leq 4.5$.

R. Feynman, Phys. Rev. Lett. **23** (1969) 1415.
R.S. Fletcher, T.K. Gaisser, P. Lipari, T. Stanev, Phys. Rev. **D50** (1994) 5710; J. Engler, T.K. Gaisser, P. Lipari, T. Stanev, Phys. Rev. **D46** (1992) 5013.
T.K. Gaisser, R.J. Protheroe, K.E. Turver, T.J.L. McComb, Rev. Mod. Phys. 50 (1978) 859.
R. Haar, C. Liapis, P. Karchin, C. Biino, S. Erhan, W. Hofmann, P. Kreuzer, D. Lynn, M. Medinnis, S. Palestini, L. Pesando, M. Punturo, P. Schlein, B. Wilkens, J. Zweizig, Phys. Lett. **B401** (1997) 176.
N.N. Kalmykov, S.S. Ostapchenko, Yad. Fiz. **56** (1993) 105; N.N. Kalmykov, S.S. Ostapchenko, Phys. At. Nucl. **56** (3) (1993) 346; N.N. Kalmykov, S.S. Ostapchenko, A.I. Pavlov, Bull. Russ. Acad. Sci. (Physics) **58** (1994) 1966.
J. Knapp, D. Heck, G. Schatz, Preprint of Forchungszentrum Karlsruhe, FZKA 5828 (1996).
C.M.G. Lattes et al. Prog. Theor. Phys. Suppl. No.47 (1971) 1.
E. Pare, T. Doke, M. Haugenauer, V. Innocente, K. Kasahara, T. Kashiwagi, J. Kikuchi, S. Lazano, K. Masuda, H. Murakami, Y. Muraki, T. Nakada, A. Nakamoto, T. Yuda, Phys Lett. **B242** (1990) 531.
J. Ranft, Phys. Rev. **D51** (1995) 64.
F.E. Taylor, D.C. Carey, J.R. Johnson, R. Kummerud, D.J. Richie, A. Roberts, J.R. Sauer, R. Shafer, D. Theriot, J.K. Walker, Phys. Rev. **D14** (1976) 1217.
K. Werner, Phys. Rep. **232** (1993) 87.